Optical Stark shift to control the dark exciton occupation of a quantum dot in a tilted magnetic field

Miriam Neumann,[1] Florian Kappe,[2] Thomas K. Bracht ,[1] Michael Cosacchi ,[3] Tim Seidelmann ,[3]
Vollrath Martin Axt,[3] Gregor Weihs ,[2] and Doris E. Reiter [1]

[1]*Institute of Solid State Theory, University of Münster, 48149 Münster, Germany*
[2]*Institute for Experimental Physics, University of Innsbruck, Innsbruck, Austria*
[3]*Theoretische Physik III, Universität Bayreuth, 95440 Bayreuth, Germany*

When a detuned and strong laser pulse acts on an optical transition, a Stark shift of the corresponding energies occurs. We analyze how this optical Stark effect can be used to prepare and control the dark exciton occupation in a semiconductor quantum dot. The coupling between the bright and dark exciton states is facilitated by an external magnetic field. Using sequences of laser pulses, we show how the dark exciton and different superposition states can be prepared. We give simple analytic formulas, which yield a good estimate for optimal preparation parameters. The preparation scheme is quite robust against the influence of acoustic phonons. We further discuss the experimental feasibility of the used Stark pulses. Giving a clear physical picture, our results will stimulate the usage of dark excitons in schemes to generate photons from quantum dots.

I. INTRODUCTION

The optical Stark effect relies on the application of a strong, detuned laser field. Applied to a few-level system as occurring in self-assembled semiconductor quantum dots (QDs), this results in an energy shift of the involved states [1]. The optical Stark effect in QDs has been used in several ways: for ultrafast control of the exciton polarization [2], to reduce the fine-structure splitting between the exciton levels [3], to induce the Autler-Towns splitting, and for spin switching in QDs doped with a single magnetic ion [4,5] to enable the preparation of Fock states in QD-cavity systems [6], to enhance and suppress the tunneling rate between double-QD structures [7], and to control the energetic landscape of a charged QD in a spin-selective manner [8]. In other systems, the Stark effect has already been used in GaAs quantum wells in 1986 [9,10], while recent applications of the Stark effect are used in 2D semiconductors [11] as well as for the ultrafast control of exciton-polariton systems [12].

In this paper, we study how the optical Stark effect can be used to address the dark exciton in a QD, which does not have an intrinsic optical dipole. We consider the dark exciton in the ground-state manifold, where the spins of the constituent electron and hole are aligned parallel, while the excitons with antiparallel spin can be optically addressed and are hence called bright excitons. While bright excitons in QDs are exploited in the usage of QDs as single-photon sources [13–17], dark excitons can be used as auxiliary states to create more complex photon states, like photonic cluster states [18] or time-bin entangled states [19,20]. Dark excitons in semiconductor materials gain more and more importance: in 2D semiconductors, it was proposed to use dark excitons as sensors [21] and in perovskite nanocrystals dark excitons can promote the photon emission rate [22].

Experimentally implemented protocols to prepare the dark ground-state exciton rely on the decay of a higher energy biexcitonic state, heralded by photon detection [23–25]. Higher-excited states addressed by a laser with a strong component along the beam axis can also relax into the dark ground-state exciton [26]. Other protocols have been proposed using a single pulse relying either on adiabatic rapid passage [27] or on phonon-assisted state preparation [28] in combination with a tilted magnetic field. A tilted magnetic field can also be used to extend the addressable states of a QD in a cavity [29,30].

In the present scheme, we propose to use two pulses to prepare the dark exciton in a QD in a tilted magnetic field: an ultrafast π-pulse to excite the bright exciton followed by a rectangular pulse with softened edges to induce the optical Stark effect. The proposed scheme has the advantage of offering a clear picture of the underlying physics to prepare the dark exciton in QDs as well as being a very precise preparation method. We provide analytical equations for the parameters of the Stark pulse, thereby offering guidance on the usage of the Stark effect. With this method, superposition states can also be easily prepared. We study the influence of acoustic phonons, which are known to often have a strong impact on exciton preparation schemes [31,32], showing that they have only a marginal influence on this preparation scheme at low temperatures. We close by discussing the experimental feasibility of the proposed Stark pulses.

II. SYSTEM AND THEORETICAL BACKGROUND

A. System states

Strongly confined QDs host discrete excitons, with their ground state being strongly separated from higher-excited

exciton states. Being composed of an electron with spin S_e and a hole with (pseudo)spin S_h, the spin combination $j = S_e + S_h$ determines the optical properties of the exciton. While the electron spin can be given by $S_e \in \{+\frac{1}{2}(\uparrow), -\frac{1}{2}(\downarrow)\}$, for holes we have to distinguish between light holes where $S_{lh} \in \{+\frac{1}{2}, -\frac{1}{2}\}$ and heavy holes with $S_{hh} \in \{+\frac{3}{2}(\Uparrow), -\frac{3}{2}(\Downarrow)\}$. In typical QDs, the heavy holes constitute the hole ground state, while the light holes are energetically separated and can be neglected [33], such that we use $S_h = S_{hh}$. We mention that for strongly strained QDs the light holes can constitute the (hole) ground states [34].

The optical selection rules can be deduced by the total spin momentum of the exciton, which can be $j = \pm 1$ or $j = \pm 2$. Emitting (absorbing) a photon requires a change of $\Delta j = \pm 1$ for circular polarization $\sigma^{\mp}$ ($\sigma^{\pm}$). This allows us to distinguish two species of excitons, depending on their ability to couple to the electromagnetic field via pair recombination (creation): Bright excitons that have antiparallel spin contributions $j = \mp S_e \pm S_h = \pm 1$ and dark excitons with parallel spin contributions $j = \pm S_e \pm S_h = \pm 2$:

$$|b^+\rangle = |\downarrow, \Uparrow\rangle \quad |b^-\rangle = |\uparrow, \Downarrow\rangle,$$
$$|d^+\rangle = |\uparrow, \Uparrow\rangle \quad |d^-\rangle = |\downarrow, \Downarrow\rangle.$$

The different excitons interact with each other via the Coulomb interaction, in particular, due to the exchange interaction. The short-range exchange interaction results in a splitting between bright and dark excitons, while the long-range exchange interaction yields an interaction between the bright excitons known as fine-structure splitting [35,36].

B. Coupling to magnetic fields

For our preparation scheme, we assume an external tilted magnetic field composed of an x and z component, which is applied to the QD. The z component of the magnetic field is helpful to adjust the energy levels in our preparation scheme as discussed below, while the x component is responsible for the coupling between bright and dark excitons, resulting in the dark exciton gaining oscillator strength and becoming bright [37]. In our model, the in-plane magnetic field mediates a spin flip of the electron only, while the hole spin remains fixed. The latter is based on the assumption that a direct spin flip between the heavy hole states is forbidden. In principle, a hole spin flip via the light hole states is possible, in particular, in the presence of band mixing, however, this process is slow compared to the preparation protocol and is further prohibited by the out-of-plane magnetic field.

In self-assembled QDs, an intrinsic coupling between bright and dark excitons can occur, e.g., via valence band mixing in highly asymmetric QDs [24,25,38] or alloy compositions [39], such that the dark exciton gains oscillator strength and becomes visible. In these cases, the dark exciton is not 100% dark anymore and recombines radiatively, but typically on a much longer timescale than the bright exciton [24]. Also, a magnetic dopant in the QD can act as an effective magnetic field on the exciton and result in spin flips [40,41].
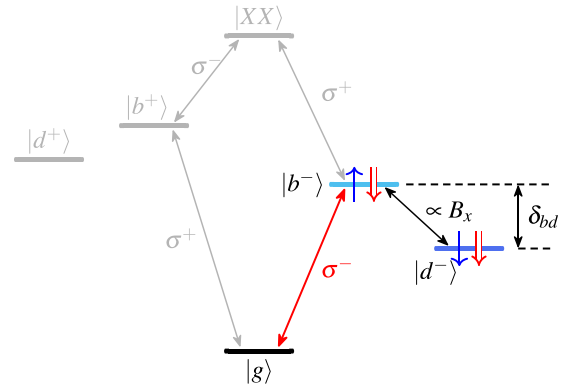

FIG. 1. Sketch of the system in the ground-state manifold of a QD including energy shifts and coupling to the light and magnetic fields. We only consider the "−" subsystem marked by color. The arrows indicate the spin configuration of the participating excitons.

C. Reduction to a three-level model

The energy levels and the most important couplings are sketched in Fig. 1. In addition to the four exciton states $|b^{\pm}\rangle$ and $|d^{\pm}\rangle$, there exist the ground state $|g\rangle$ with no excitation and the biexciton state $|XX\rangle$. Due to the bright-dark splitting and the energy shifts induced by the z component of the magnetic field, all single-exciton states are at different energies. The figure also depicts the optical selection rules for circularly polarized pulses.

Assuming an excitation with only σ^--polarized light, we can reduce our system to a three-level system consisting of $\{|g\rangle, |b^-\rangle, |d^-\rangle\} \equiv \{|g\rangle, |b\rangle, |d\rangle\}$. While, in principle, the two bright excitons would be coupled via the fine-structure splitting, for typical splittings of a few tens of μeV [42], the conversion is much slower than our preparation scheme and gets further suppressed due to the magnetic field. As such, a preparation into the biexciton state is not feasible for a given circular polarization.

The Hamiltonian can then be written as

$$H = H_0(B_z) + H_{\text{flip}}(B_x) + H_{\text{light}}, \tag{1}$$

with H_0 accounting for the energies of the above electronic states in the out-of-plane magnetic field B_z, H_{flip} for the spin flips induced by the in-plane magnetic field B_x and H_{light} for the coupling to the light field. For the three levels, $H_0(B_z)$ reads

$$H_0(B_z) = \hbar\omega_0 |b\rangle\langle b| + (\hbar\omega_0 - \delta_{bd})|d\rangle\langle d|, \tag{2}$$

where the energy of the ground state is set to zero, $\hbar\omega_0$ is the energy of the bright state, and the dark state is shifted by δ_{bd}. The energy splitting between bright and dark states is determined by the intrinsic bright-dark splitting δ_0 and can be adjusted by the z component of the magnetic field B_z, such that the effective splitting reads $\delta_{bd}(B_z) = \delta_0 - g_{e,z} \mu_B B_z$. μ_B is the Bohr magneton. Because the two exciton states differ just by their electron spin component, here only the electron g factor $g_{e,z}$ enters.

The in-plane magnetic field B_x can result in a spin-flip of the electron, which couples bright and dark excitons,

$$H_{\text{flip}}(B_x) = -\frac{J}{2}|b\rangle\langle d| + \text{H.c.}, \tag{3}$$

via the coupling constant $J(B_x) = g_{\text{e},x}\,\mu_B\,B_x$.

The interaction with the light field is treated in the dipole and rotating wave approximation reading

$$H_{\text{light}} = -\frac{\hbar}{2}\Omega(t)|b\rangle\langle g| + \text{H.c.} \tag{4}$$

The electric field is given by $\Omega(t)$. We will consider two types of pulses:

$$\Omega_P(t) = \frac{\theta}{\sqrt{2\pi}\,\tau}e^{-t^2/(2\tau^2)}e^{-i\omega_P t}, \tag{5}$$

$$\Omega_S(t) = \frac{\Omega_0}{(1 + e^{-\alpha\cdot t})(1 + e^{-\alpha\cdot(\tau_S - t)})}e^{-i\omega_S t}. \tag{6}$$

On the one hand, we consider short laser pulses with a Gaussian envelope which are characterized by their pulse area θ and $\tau = 0.15$ ps. The carrier frequency of this laser pulse is set to be resonant with the transition frequency to the bright exciton $\omega_P = \omega_0$. In addition, we consider Stark pulses which have an essentially constant amplitude Ω_0 during their length τ_S. We assume that the Stark pulse has softened edges with a rise time of $1/\alpha = 0.1$ ps. The carrier frequency of the Stark pulses is detuned from the transition frequency. To shift the eigenenergies of the system to lower values, we have to use a positive detuning, which is given by $\Delta = \omega_S - \omega_0$.

To compute the time evolution, we use the density matrix formalism and numerically integrate the von Neumann equation. Initially, we take the system to be in the ground state $|g\rangle$.

During the Stark pulse, we can write the Hamiltonian in matrix form in the basis $(|g\rangle, |b\rangle, |d\rangle)$ as

$$\tilde{H} = \begin{pmatrix} \hbar\Delta & -\frac{\hbar}{2}\Omega_0 & 0 \\ -\frac{\hbar}{2}\Omega_0 & 0 & -\frac{1}{2}J \\ 0 & -\frac{1}{2}J & -\delta_{bd} \end{pmatrix}. \tag{7}$$

Here we have chosen a frame where the exciton energy becomes zero, while the ground-state energy is given by the detuning. Note that this frame differs from typical rotating frames but allows us an intuitive interpretation of the results. By diagonalization of this matrix, we obtain the energy eigenstates of the system E_i, which we refer to as dressed states $|i\rangle$ with $i \in \{1, 2, 3\}$ in the following. While we perform the calculations in the bare state basis, the dressed states are useful for the interpretation of the dynamics.

D. Optical Stark effect

In a two-level system composed of the optically active states $|g\rangle$ and $|b\rangle$, the action of the Stark pulse can be calculated by diagonalization of the corresponding Hamiltonian in the rotating frame:

$$\tilde{H} = \begin{pmatrix} \hbar\Delta & -\frac{\hbar}{2}\Omega_0 \\ -\frac{\hbar}{2}\Omega_0 & 0 \end{pmatrix}. \tag{8}$$

Note that we here set $J = 0$ to focus on the optical Stark effect, such that we can omit the third state from Eq. (7). The
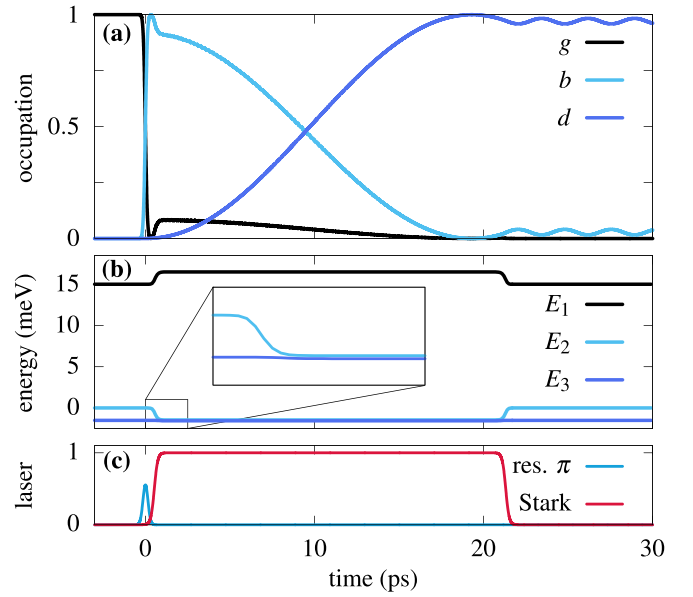

FIG. 2. (a) Dynamics of the occupations g, b, and d of the states in the three-level system, (b) evolution of the dressed-state energies E_i and (c) sequence of the laser fields. Parameters for this example are $\hbar\Delta = 15$ meV, $\delta_{bd} = 1.5$ meV and $\hbar\Omega_0 = 9.95$ meV.

diagonalization yields the eigenenergies:

$$E_\pm(\Omega_0) = \frac{\hbar}{2}\Delta \pm \frac{\hbar}{2}\sqrt{\Delta^2 + \Omega_0^2}. \tag{9}$$

From this equation, it is evident that applying a laser introduces an additional energetic splitting of the two eigenstates, which are now mixtures of the original ones. The Stark shift induced by the light field can be written as

$$\Delta E_{\text{Stark}} = |E_\pm(\Omega_0) - E_\pm(0)|. \tag{10}$$

Even with the in-plane magnetic field ($J \neq 0$), the influence of the third level $|d\rangle$ is negligible in most of the cases considered here. On the one hand, it is optically inactive and hence no direct coupling to the Stark pulse is possible. On the other hand, the dark state gains some optical activity, which makes it subject to the influence of the Stark pulse, but we assume in most cases that the coupling J is much smaller than the bright-dark spitting δ_{bd}, making this contribution very small.

III. PREPARATION SCHEMES

Next, we will use pulse sequences to prepare different states in a GaAs QD. We set the coupling constant to $J = 0.11$ meV, which for an electronic g factor of $g_{\text{e},x} = -0.65$ [37] corresponds to an in-plane magnetic field of $B_x = -3$ T. If not denoted otherwise, we use a bright-dark splitting of $\delta_{bd} = 1.5$ meV to illustrate our schemes.

A. Preparation of the dark exciton

We start by proposing a method for preparing the dark exciton state using the optical Stark effect, i.e., we aim for a high occupation of the dark exciton $|d\rangle$ after the application of the Stark pulse. In Fig. 2, the dynamics of (a) the occupations g, b, and d of the involved states, (b) the corresponding

dressed-state energies, and (c) the used pulse sequence are shown.

In the beginning, the system is in the ground state. By means of a π pulse applied at $t = 0$, which is resonant with the transition between the ground state and the bright exciton, the occupation switches completely to the bright exciton. After this, the off-resonant Stark pulse is switched on. The Stark pulse is a flat pulse that is positively detuned by $\hbar\Delta = 15$ meV with respect to the transition between the ground state and the bright exciton. During the Stark pulse, the bright-state population diminishes in favor of the dark-state population, which almost rises to unity. At $t \approx 21$ ps, we turn off the Stark pulse and small oscillations between the bright and dark state occupation remain.

During the action of the Stark pulse, the bright and dark exciton states are shifted into resonance. The behavior can also be understood by looking at the dressed-state energies as shown in Fig. 2(b). Without the Stark pulse, E_1 corresponds to the ground state $|g\rangle$, E_2 to the bright state $|b\rangle$, and E_3 to the dark state $|d\rangle$. The Stark pulse now brings E_2 and E_3 close together and diabatic transitions between them take place. To preserve maximum dark-state occupation, the Stark pulse is switched off when the occupation reaches its maximum, such that the eigenstates again shift out of resonance. Because the two excitons are still coupled via the magnetic field, the system continues with a small, off-resonant oscillation.

We now want to quantify the parameters for a Stark pulse that leads to a high occupation of the dark exciton. For this, we first analyze the condition that brings the bright and dark exciton states into resonance. To this end, we vary the detuning and amplitude of the Stark pulse and calculate the mean occupation of the dark exciton after the pulse as shown in Fig. 3(a). We see that there is a clear condition for a high population of the dark exciton. This can be quantified by assuming that the energy shift induced by the optical Stark effect should be equal to the bright-dark splitting, leading to the resonance condition (for the case $\Delta > 0$ considered in this paper):

$$\delta_{bd} \overset{!}{=} |\Delta E_{\text{Stark}}| = \left| \frac{\hbar}{2}\Delta - \frac{\hbar}{2}\sqrt{\Delta^2 + \Omega_0^2} \right|. \quad (11)$$

From this, we derive for the mean occupation of the dark exciton

$$
\begin{aligned}
d_{\text{final}} &= d_{\text{max}} - d_{\text{osc}} \\
&= \frac{J^2}{J^2 + (\delta_{bd} - |\Delta E_{\text{Stark}}|)^2} - \frac{1}{2}\frac{J^2}{J^2 + \delta_{bd}^2}.
\end{aligned}
\quad (12)
$$

Here, d_{max} is the maximal occupation during the Stark pulse, which in the resonant case is $d_{\text{max}} = 1$. Due to the switch-off and the residual oscillation, this maximal occupation is reduced by the second term d_{osc}. This model yields a good approximation of the numerical results as can be seen by the red dashed line in Fig. 3(a), marking the analytic position of d_{max}.

Furthermore, from the period of the oscillation between the bright and dark exciton states, we can derive the length of the
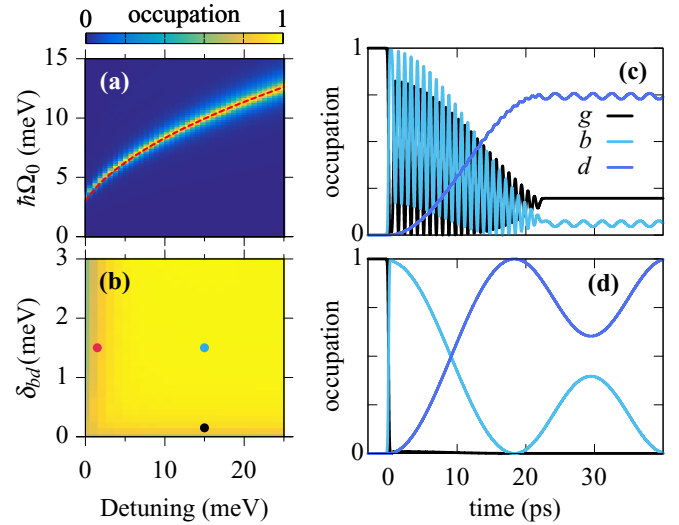

FIG. 3. (a) Mean occupation of the dark exciton state after the action of the Stark pulse as function of detuning and strength of the Stark pulse $\hbar\Omega_0$ for a bright-dark splitting of $\delta_{bd} = 1.5$ meV. The red dashed line indicates Eq. (11). (b) Final occupation as function of detuning and effective bright-dark splitting. The colored dots indicate the parameters shown in the examples of the dynamics shown on the right (red and black) and in Fig. 2 (blue). (c), (d) Occupations g, b, and d in the three-level system (c) for detuning $\hbar\Delta = 1.5$ meV bright dark-splitting $\delta_{bd} = 1.5$ meV and $\hbar\Omega_0 = 4.24$ meV [red dot in (b)] and (d) $\hbar\Delta = 15$ meV, $\delta_{bd} = 0.15$ meV and $\hbar\Omega_0 = 3.01$ meV [black dot in (b)].

Stark pulse necessary for the state preparation as

$$\tau_S = \frac{(2n+1)\pi\hbar}{\sqrt{J^2 + (\delta_{bd} - |\Delta E_{\text{Stark}}|)^2}}, \quad n \in \mathbb{N}_0. \quad (13)$$

Besides the pulse strength, the bright-dark splitting is also a crucial input parameter. Figure 3(b) shows the occupation of the dark exciton as a function of detuning and bright-dark splitting δ_{bd}. In all cases, we choose the strength Ω_0 of the Stark pulse according to the resonance condition Eq. (11). For most parameters, a near-unity occupation can be achieved. Only for small detunings and small bright-dark splittings, the preparation of the dark exciton is limited. In a GaAs QD, the typical intrinsic bright-dark splitting is $\delta_0 = 0.25$ meV [35]. To achieve the chosen bright-dark splitting of $\delta_{bd} = 1.5$ meV, with an electronic g factor of $g_{e,z} = -0.8$ [43], this would refer to an out-of-plane magnetic field of $B_z = 27$ T. For a more realistic value of $B_z = 4$ T, we obtain $\delta_{bd} = 0.43$ meV and an optimal value of $\hbar\Omega_0 = 5.15$ meV, which also results in an occupation close to unity with an average occupation of 0.95 [see also Fig. 3(b)]

For a given in-plane magnetic field, the ratio between bright-dark splitting and coupling constant J also determines the optical activity of the dark exciton. Therefore, in a linear absorption spectrum, two peaks appear. While at vanishing δ_{bd} these peaks have equal strength, for a finite δ_{bd} a peak close to E_d and a peak close to E_b appears with different strengths. Taking as an example $\delta_{bd} = 0.43$ meV and $J = 0.11$ meV, we find that the amplitude of the peak at E_d is 0.0016 of the one at E_b, showing that for these values the dark exciton remains
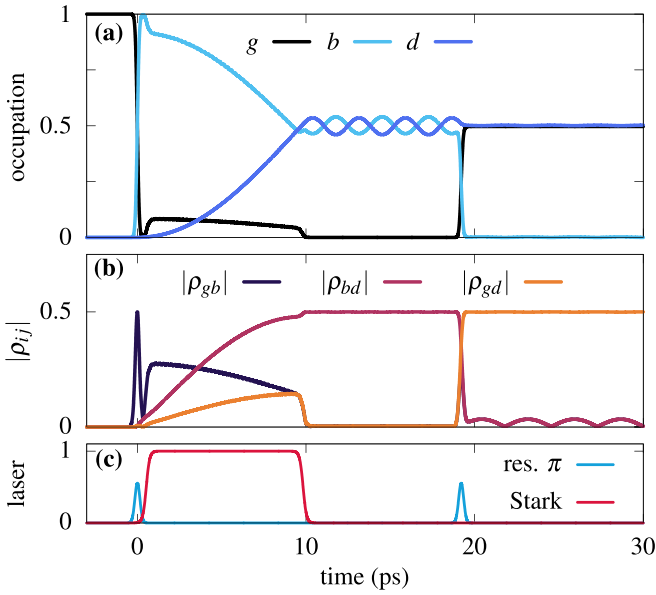
FIG. 4. Dynamics of (a) occupations g, b, d of the states in the three-level system and (b) the coherences ρ_{ij} with $i, j \in \{g, b, d\}$ under (c) the laser sequence. Same parameters as in Fig. 2.

mostly dark. This is crucial for the success of the preparation protocol.

Two examples for nonoptimal preparation are shown in Figs. 3(c) and 3(d). In Fig. 3(c), we consider the case where the detuning $\hbar\Delta = 1.5$ meV is too small to ensure a close to unity preparation. Because of the small detuning, the Stark pulse still induces a strong oscillation between ground and bright exciton state. This hinders the oscillation between bright and dark excitons, such that after the pulse only an occupation of about 0.75 is achieved and the ground state is strongly occupied. In Fig. 3(d), the bright-dark splitting is set to $\delta_{bd} = 0.15$ meV. Here we find that after the Stark pulse, we still see a strong oscillation between bright and dark excitons, hence the median occupation is clearly below one. This is an important aspect to the necessity of the application of a magnetic field with a z component. Taking just a magnetic field with in-plane direction would result in a bright-dark splitting equal to the intrinsic splitting. In typical GaAs QDs this splitting is often too small to ensure a high-fidelity preparation.

B. Preparation of superposition states

The possibility to switch between bright and dark states in a deterministic and precise fashion allows us to prepare different superposition states within the three-level system (cf. Fig. 1). An example of creating a superposition state is shown in Fig. 4, which displays (a) the occupations of the states alongside (b) the coherences ρ_{ij} for (c) a laser pulse sequence consisting of a π-pulse, a Stark pulse and a second π-pulse.

The sequence starts the same way as the dark exciton preparation scheme, but this time we switch off the Stark pulse after half the time at $t \approx 10$ ps, where the bright and dark states have a similar occupation of about 0.5. As before,

due to the in-plane magnetic field after the switch-off, there is a small oscillation on the occupations. It is interesting to follow the dynamics of the coherences. Due to the switch-on of the Stark pulse, the coherence between ground and bright state $|\rho_{gb}|$ rises. Then, during the Stark pulse, we see that the coherence between bright and dark exciton $|\rho_{bd}|$ builds up. Also the coherence between ground and dark state ρ_{gd} increases. This behavior can be traced back to the composition of the involved dressed states $|2\rangle$ and $|3\rangle$, which are a mixture of all bare states. When switching off the Stark pulse, both $|\rho_{gb}|$ and $|\rho_{gd}|$ go to zero and we obtain the superposition:

$$|\psi\rangle_{bd} = \frac{1}{\sqrt{2}}\left(|b\rangle + e^{-i\omega_{bd}t}e^{i\varphi_{bd}}|d\rangle\right). \tag{14}$$

The coherence between $|b\rangle$ and $|d\rangle$ oscillates with the respective energy difference, i.e., with $\omega_{bd} = \delta_{bd}/\hbar$. During the protocol, the coherence gains an additional phase $\varphi_{bd} = -\pi/2$. After some waiting time, we apply a second π-pulse to deexcite the bright exciton to obtain the superposition state:

$$|\psi\rangle_{gd} = \frac{1}{\sqrt{2}}\left(|g\rangle + e^{i(\omega_0 - \omega_{bd})t}e^{i\varphi_{gd}}|d\rangle\right). \tag{15}$$

The coherence of $|\psi\rangle_{gd}$ oscillates with the energy difference between $|g\rangle$ and $|d\rangle$ with an additional phase φ_{gd} gained during the action of the π-pulse. Note that if we were to wait for the spontaneous decay of the bright exciton, we would also expect to obtain the superposition state $|\psi\rangle_{gd}$, just with a different phase. The preparation of superposition states consisting of three or four energy levels are highly interesting for the generation of photonic cluster states [18,44]. In our case, a superposition of photons in different time bins could be created by successive deexcitation of the dark exciton by Stark pulses inducing only partial back-conversion to the bright exciton.

IV. INFLUENCE OF PHONONS

In QDs, phonons can strongly modify the state preparation schemes compared to the atomic case [31–33,45]. In the following, we therefore take into account the coupling to longitudinal acoustic (LA) phonons, known to be the most important source of decoherence at low temperatures.

A. Exciton-phonon interaction

The coupling to phonons is treated in the standard way via the Hamiltonian

$$H_{\text{ph}} = \hbar \sum_{\mathbf{q}} \omega_{\mathbf{q}} b_{\mathbf{q}}^{\dagger} b_{\mathbf{q}}$$
$$+ \hbar(|b\rangle\langle b| + |d\rangle\langle d|) \sum_{\mathbf{q}} \left(g_{\mathbf{q}} b_{\mathbf{q}} + g_{\mathbf{q}}^{*} b_{\mathbf{q}}^{\dagger}\right), \tag{16}$$

where $b_{\mathbf{q}}^{\dagger}$ ($b_{\mathbf{q}}$) is the bosonic creation (annihilation) operator for phonons with energy $\hbar\omega_{\mathbf{q}}$ that are coupled to the QD exciton states by $g_{\mathbf{q}}$. We assume a linear dispersion for the LA phonons and typical GaAs parameters [28] at $T = 1$ K with a spectral density of a spherical QD with radius of 3 nm [46].

When included in the equations of motion, the exciton-phonon interaction leads to the well-known infinite hierarchy

of equations of motions, which we here truncate using a fourth-order correlation expansion formalism [47]. It has been shown that for standard GaAs-QD coupling parameters at not too high temperatures, this method yields results coinciding with those given by numerically exact approaches such as the path integral formalism [48–50] and a good agreement with experiment [51].

Most importantly, the correlation expansion includes renormalization effects due to phonons as well as relaxation processes between the dressed states. It further describes effects of non-Markovian dynamics [45,52]. The phonon renormalization of the excitonic energies is known as polaron shift and is given by

$$\hbar\omega_0 \rightarrow \hbar\omega_0 - \hbar\Omega_{\mathrm{pol}} = \hbar\omega_0 - \hbar\sum_{\mathbf{q}} \frac{|g_{\mathbf{q}}|^2}{\omega_{\mathbf{q}}}. \quad (17)$$

It is a result of the formation of a polaron quasiparticle. Note that the polaron shift is the same for bright and dark exciton, such that the bright-dark splitting is not affected. For the optical transition, to match the resonance condition, the polaron shift $\hbar\Omega_{\mathrm{pol}}$ has to be taken into account. This is much smaller than the separation to the next excited state ($\gtrsim 65\,\mathrm{meV}$ [53]), such that the considered three-level approach still holds. Because the phonons also change the Rabi frequency between ground and bright exciton state [47,54,55], the pulse areas also have to be readjusted.

B. Impact on preparation protocols

To assess the impact of the phonon environment on our preparation protocol, we repeat the same protocols as in Sec. III, now accounting for the exciton-phonon interaction by using adjusted energies and pulse areas. Figure 5(a) shows the occupation of the involved states for the dark-state preparation for $T = 1\,\mathrm{K}$. Similar to Fig. 2, we find that after the pulses the dark exciton occupation is again close to unity. The marginal influence of the phonons can be understood by considering the relaxation processes induced by phonons in the dressed state basis [see Fig. 2(b)]. The dynamics start initially in $|2\rangle$, i.e., the middle dressed state, with diabatic transitions occurring to the lower dressed state. At low temperatures, the phonons can only lead to a transition from higher to lower lying dressed states due to phonon emission [56], while phonon absorption is highly unlikely. However, due to the mixing coefficients and the large energy difference between the states, even the former transitions are highly unlikely. Hence, the phonons do not disturb the preparation scheme. The main difference in the case with phonons is a high-frequency oscillation with a small amplitude on top of the ground and bright exciton occupation as observed in Fig. 5(a). The origin of these oscillations is the phonon damping during the π-pulse, which results in a nonunity preparation of the bright exciton. Accordingly, also a superposition of the dressed states $|1\rangle$ and $|3\rangle$ occurs, where the high-energy splitting between them corresponds to the frequency of the fast oscillations.

Also, phonons do not noticeably disturb the preparation of the superposition state. The corresponding calculation with phonons at $T = 1\,\mathrm{K}$ is shown in Fig. 5(c), which shows similar occupations to the phonon-free case [cf. Fig. 4]. As
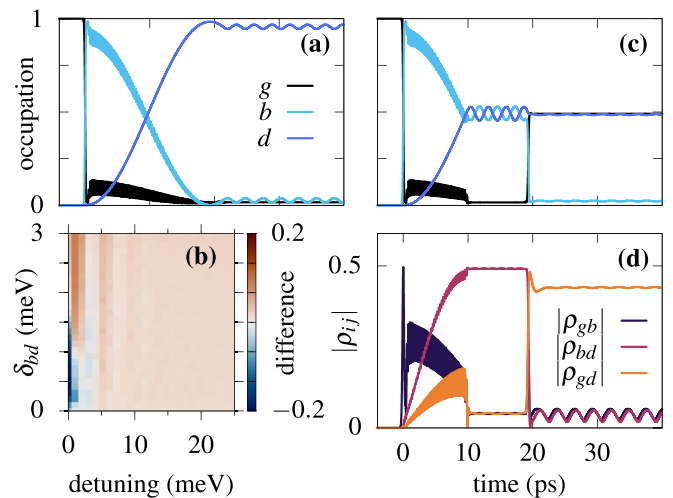

FIG. 5. Dynamics of the occupation including the exciton-phonon interaction for $T = 1\,\mathrm{K}$ for (a) the dark-state preparation scheme [cf. Fig. 2] and (c) the preparation of the superposition [cf. Fig. 4]. (d) Dynamics of the coherences including the exciton-phonon interaction for the preparation into the superposition state in (c). (b) Difference of the final occupation without phonons [cf. Fig. 3(b)] to the case including phonons as a function of detuning and bright-dark splitting. Note that a blue hue indicates a phonon enhancement of the preparation fidelity.

the phonon environment is well known to dampen the Rabi rotations in the two-level system [31,47,57], it is interesting to analyze whether they affect the coherences. However, as demonstrated in Fig. 5(d), the coherences are also mostly unaffected by the phonons.

To summarize the influence of phonons, Fig. 5(b) shows the difference of the final dark-state occupation between calculations without and with phonons. For a wide range of excitation conditions, quantified by the laser detuning, and a variety of dark-bright splittings, the difference is in the percentage range and thus very small. Only at small detunings, where the amplitude of these oscillations is high, the damping by phonons is especially effective, because here strong oscillations between ground and bright exciton states take place, which are highly affected by phonons. Therefore, the final occupation of the dark state is also affected, since our protocol relies on the bright state's occupation as an intermediary. It is noteworthy that there are not only regions where the final dark-state occupation is dampened by phonons, but also regions of phonon enhancement can be found [blue-hued areas in Fig. 5(b)]. In this region, the energetic splitting between the eigenenergies E_1 and E_2 is in the range of the phonon spectral density, which has its maximum at 2 meV for our parameter set. This leads to phonon-assisted transitions [28] from the ground state to the bright exciton state and therefore supports the preparation of the dark exciton.

For very high detunings, the splitting between the dressed states $|1\rangle$ and $|2\rangle$, which have mainly ground state and exciton characteristics, can surpass the phonon spectral density and phonon processes can be completely suppressed [51]. In these regions, our preparation protocol also becomes stable against phonon influence at higher temperatures.
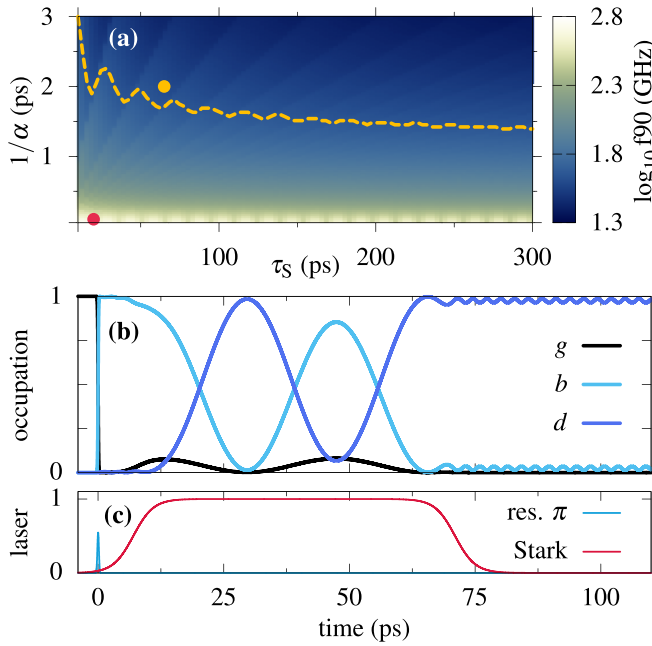
FIG. 6. (a) Classification of the electric driving signal as a function of $1/\alpha$ and τ_S. Colors indicate the frequency where 90% of the electrical driving signal is present (f90). Orange dashed line: 45 GHz line for modern EOM systems. The dots indicate the value used for the dark state preparation (red: Fig. 2; orange: this figure). (b) Dynamics of the occupation of the three-level system without phonons for the pulse sequence shown in (c). Parameters for this example are $\hbar\Delta = 15$ meV, $\delta_{bd} = 1.5$ meV, and $\hbar\Omega_0 = 10.1$ meV.

V. EXPERIMENTAL FEASIBILITY OF STARK PULSES

The shown method relies on the application of two different kinds of laser pulses, a resonant π pulse followed by a spectrally detuned Stark pulse. Exciton preparation via resonant π pulses has already been demonstrated many times [58,59] and provides no new experimental challenge since one can use commercially available pulsed laser systems that can provide pulse durations of the order of 100 fs. However, generating a laser pulse of the form presented in Eq. (6) requires more attention.

One straightforward way of generating such pulses is to utilize fast electro-optical modulators (EOMs) and cut the desired pulses from a continuous wave laser source operating at the desired wavelength. A clear advantage of this method is that one can use the π pulse and a sufficiently fast photodiode as a trigger to start the driving signal for the EOM, which is much easier than synchronizing two pulsed laser sources.

Commercially available EOM systems nowadays support a bandwidth of up to 45 GHz which restricts the experimentally possible values of α and τ_S in Eq. (6). Sweeping these parameters, calculating the respective electrical bandwidth, and integrating to a point where 90% of the driving signal's frequency contributions are present allows us to check for possible values for α and τ_S as shown in Fig. 6(a).

As evident from Fig. 6(a), there exists a limit for the experimentally realizable values of α and τ_S using currently available EOMs, which is indicated by the orange dashed line. In particular, everything above this orange line can be realized with current EOMs. The red dot indicates the present parameters of the Stark pulse as used in Fig. 2 with $1/\alpha = 0.1$ ps and a length of about 20 ps. We find that these parameters are strongly below what is currently achievable in experiments.

To achieve a feasible length of the Stark pulse, we need to use much longer pulses of several tens of ps. This can be done in several ways. One possibility would be to reduce the in-plane magnetic field B_x and, accordingly, lengthen the period of the oscillation between bright and dark exciton states. Another opportunity is to wait for more than one half period to switch off the Stark pulse. The second aspect is, that even for a longer pulse length, the rise time of the Stark pulse has to be increased, such that it is on the order of a few ps.

To test if our proposed methods still work for such less favorable pulse parameters, Figs. 6(b) and 6(c) show the population dynamics and laser sequence for currently realizable experimental parameters: $1/\alpha = 2$ ps and $\tau_S = 64$ ps [orange dot in Fig. 6(a)]. We take the same magnetic field values as in Fig. 2 and wait for one and a half oscillations to take place before switching off the pulse. In the case without phonons, the longer rise time and Stark pulse length also leads to a near-unity population of the dark exciton state, utilizing one and a half oscillations of the induced dark-bright splitting. These preparation times are still short compared to the lifetime of the bright exciton, which is on a timescale of several hundred of ps up to a ns [60], therefore we think that even when using longer pulses our proposed scheme is still feasible.

VI. CONCLUSION

In summary, we have analyzed the usage of the optical Stark effect to prepare and control the dark-state excitation for a QD in a tilted magnetic field. The Stark effect allows preparation of the dark exciton with almost unity fidelity, even under the influence of phonons. By adjusting the length of the Stark pulse, we can prepare different superposition states, including the dark exciton. Coherent control of the dark-state occupation can be useful to enhance already existing or establish new preparation protocols in QDs to generate new light states like entangled or cluster states.

[1] G. Jundt, L. Robledo, A. Högele, S. Fält, and A. Imamoğlu, Observation of Dressed Excitonic States in a Single Quantum Dot, Phys. Rev. Lett. **100**, 177401 (2008).

[2] T. Unold, K. Mueller, C. Lienau, T. Elsaesser, and A. D. Wieck, Optical Stark Effect in a Quantum Dot: Ultrafast Control of Single Exciton Polarizations, Phys. Rev. Lett. **92**, 157401 (2004).

[3] A. Muller, W. Fang, J. Lawall, and G. S. Solomon, Creating Polarization-Entangled Photon Pairs from a Semiconductor Quantum Dot Using the Optical Stark Effect, Phys. Rev. Lett. **103**, 217402 (2009).

[4] C. Le Gall, A. Brunetti, H. Boukari, and L. Besombes, Optical Stark effect and Dressed Exciton States in a Mn-Doped CdTe Quantum Dot, Phys. Rev. Lett. **107**, 057401 (2011).

[5] D. E. Reiter, T. Kuhn, and V. M. Axt, Spin switching in a Mn-doped quantum dot using the optical Stark effect, Phys. Rev. B **85**, 045308 (2012).

[6] M. Cosacchi, J. Wiercinski, T. Seidelmann, M. Cygorek, A. Vagov, D. E. Reiter, and V. M. Axt, On-demand generation of higher-order Fock states in quantum-dot–cavity systems, Phys. Rev. Research **2**, 033489 (2020).

[7] N. Tsukada, M. Gotoda, T. Isu, M. Nunoshita, and T. Nishino, Dynamical control of quantum tunneling due to ac Stark shift in an asymmetric coupled quantum dot, Phys. Rev. B **56**, 9231 (1997).

[8] T. A. Wilkinson, D. J. Cottrill, J. M. Cramlet, C. E. Maurer, C. J. Flood, A. S. Bracker, M. Yakes, D. Gammon, and E. B. Flagg, Spin-selective AC Stark shifts in a charged quantum dot, Appl. Phys. Lett. **114**, 133104 (2019).

[9] A. V. Lehmen, D. S. Chemla, J. E. Zucker, and J. P. Heritage, Optical Stark effect on excitons in GaAs quantum wells, Opt. Lett. **11**, 609 (1986).

[10] A. Mysyrowicz, D. Hulin, A. Antonetti, A. Migus, W. T. Masselink, and H. Morkoç, "Dressed Excitons" in a Multiple-Quantum-Well Structure: Evidence for an Optical Stark Effect with Femtosecond Response Time, Phys. Rev. Lett. **56**, 2748 (1986).

[11] P. D. Cunningham, A. T. Hanbicki, T. L. Reinecke, K. M. McCreary, and B. T. Jonker, Resonant optical Stark effect in monolayer WS 2, Nat. Commun. **10**, 5539 (2019).

[12] D. Panna, N. Landau, L. Gantz, L. Rybak, S. Tsesses, G. Adler, S. Brodbeck, C. Schneider, S. Höfling, and A. Hayat, Ultrafast manipulation of a strongly coupled light–matter system by a giant ac Stark effect, ACS Photon. **6**, 3076 (2019).

[13] X. Ding, Y. He, Z.-C. Duan, N. Gregersen, M.-C. Chen, S. Unsleber, S. Maier, C. Schneider, M. Kamp, S. Höfling, C.-Y. Lu, and J.-W. Pan, On-Demand Single Photons with High Extraction Efficiency and Near-Unity Indistinguishability from a Resonantly Driven Quantum Dot in a Micropillar, Phys. Rev. Lett. **116**, 020401 (2016).

[14] N. Somaschi, V. Giesz, L. De Santis, J. C. Loredo, M. P. Almeida, G. Hornecker, S. L. Portalupi, T. Grange, C. Antón, J. Demory, C. Gómez, I. Sagnes, N. D. Lanzillotti-Kimura, A. Lemaítre, A. Auffeves, A. G. White, L. Lanco, and P. Senellart, Near-optimal single-photon sources in the solid state, Nat. Photon. **10**, 340 (2016).

[15] L. Schweickert, K. D. Jöns, K. D. Zeuner, S. F. Covre da Silva, H. Huang, T. Lettner, M. Reindl, J. Zichi, R. Trotta, A. Rastelli, and V. Zwiller, On-demand generation of background-free single photons from a solid-state source, Appl. Phys. Lett. **112**, 093106 (2018).

[16] L. Hanschke, K. A. Fischer, S. Appel, D. Lukin, J. Wierzbowski, S. Sun, R. Trivedi, J. Vučković, J. J. Finley, and K. Müller, Quantum dot single-photon sources with ultra-low multi-photon probability, npj Quantum Inf. **4**, 43 (2018).

[17] M. Cosacchi, F. Ungar, M. Cygorek, A. Vagov, and V. M. Axt, Emission-Frequency Separated high Quality Single-Photon Sources Enabled by Phonons, Phys. Rev. Lett. **123**, 017403 (2019).

[18] I. Schwartz, D. Cogan, E. R. Schmidgall, Y. Don, L. Gantz, O. Kenneth, N. H. Lindner, and D. Gershoni, Deterministic generation of a cluster state of entangled photons, Science **354**, 434 (2016).

[19] H. Jayakumar, A. Predojević, T. Kauten, T. Huber, G. S. Solomon, and G. Weihs, Time-bin entangled photons from a quantum dot, Nat. Commun. **5**, 4251 (2014).

[20] T. Huber, L. Ostermann, M. Prilmüller, G. S. Solomon, H. Ritsch, G. Weihs, and A. Predojević, Coherence and degree of time-bin entanglement from quantum dots, Phys. Rev. B **93**, 201301(R) (2016).

[21] M. Feierabend, G. Berghäuser, A. Knorr, and E. Malic, Proposal for dark exciton based chemical sensors, Nat. Commun. **8**, 14776 (2017).

[22] P. Tamarat, L. Hou, J.-B. Trebbia, A. Swarnkar, L. Biadala, Y. Louyer, M. I. Bodnarchuk, M. V. Kovalenko, J. Even, and B. Lounis, The dark exciton ground state promotes photon-pair emission in individual perovskite nanocrystals, Nat. Commun. **11**, 6001 (2020).

[23] E. Poem, Y. Kodriano, C. Tradonsky, N. H. Lindner, B. D. Gerardot, P. M. Petroff, and D. Gershoni, Accessing the dark exciton with light, Nat. Phys. **6**, 993 (2010).

[24] I. Schwartz, E. R. Schmidgall, L. Gantz, D. Cogan, E. Bordo, Y. Don, M. Zielinski, and D. Gershoni, Deterministic Writing and Control of the Dark Exciton Spin Using Single Short Optical Pulses, Phys. Rev. X **5**, 011009 (2015).

[25] T. Heindel, A. Thoma, I. Schwartz, E. R. Schmidgall, L. Gantz, D. Cogan, M. Strauß, P. Schnauber, M. Gschrey, J.-H. Schulze *et al.*, Accessing the dark exciton spin in deterministic quantum-dot microlenses, APL Photon. **2**, 121303 (2017).

[26] M. Holtkemper, G. F. Quinteiro, D. E. Reiter, and T. Kuhn, Dark exciton preparation in a quantum dot by a longitudinal light field tuned to higher exciton states, Phys. Rev. Research **3**, 013024 (2021).

[27] S. Lüker, T. Kuhn, and D. E. Reiter, Direct optical state preparation of the dark exciton in a quantum dot, Phys. Rev. B **92**, 201305(R) (2015).

[28] S. Lüker, T. Kuhn, and D. E. Reiter, Phonon-assisted dark exciton preparation in a quantum dot, Phys. Rev. B **95**, 195305 (2017).

[29] C. A. Jiménez-Orjuela, H. Vinck-Posada, and J. M. Villas-Bôas, Dark excitons in a quantum-dot–cavity system under a tilted magnetic field, Phys. Rev. B **96**, 125303 (2017).

[30] C. A. Jiménez-Orjuela, H. Vinck-Posada, and J. M. Villas-Bôas, Strong coupling of two quantum dots with a microcavity in the presence of an external and tilted magnetic field, Physica B **585**, 412070 (2020).

[31] A. J. Ramsay, A. V. Gopal, E. M. Gauger, A. Nazir, B. W. Lovett, A. M. Fox, and M. S. Skolnick, Damping of exciton Rabi Rotations by Acoustic Phonons in Optically Excited InGaAs/GaAs Quantum Dots, Phys. Rev. Lett. **104**, 017402 (2010).

[32] S. Lüker and D. E. Reiter, A review on optical excitation of semiconductor quantum dots under the influence of phonons, Semicond. Sci. Technol. **34**, 063002 (2019).

[33] D. E. Reiter, T. Kuhn, M. Glässl, and V. M. Axt, The role of phonons for exciton and biexciton generation in an optically

driven quantum dot, J. Phys.: Condens. Matter **26**, 423203 (2014).

[34] Y. H. Huo, B. J. Witek, S. Kumar, J. R. Cardenas, J. X. Zhang, N. Akopian, R. Singh, E. Zallo, R. Grifone, D. Kriegner *et al.*, A light-hole exciton in a quantum dot, Nat. Phys. **10**, 46 (2014).

[35] M. Bayer, G. Ortner, O. Stern, A. Kuther, A. A. Gorbunov, A. Forchel, P. Hawrylak, S. Fafard, K. Hinzer, T. L. Reinecke, S. N. Walck, J. P. Reithmaier, F. Klopf, and F. Schäfer, Fine structure of neutral and charged excitons in self-assembled In(Ga)As/(Al)GaAs quantum dots, Phys. Rev. B **65**, 195315 (2002).

[36] D. Gammon, E. S. Snow, B. V. Shanabrook, D. S. Katzer, and D. Park, Fine Structure Splitting in the Optical Spectra of Single GaAs Quantum Dots, Phys. Rev. Lett. **76**, 3005 (1996).

[37] M. Bayer, O. Stern, A. Kuther, and A. Forchel, Spectroscopic study of dark excitons in $In_xGa_{1-x}As$ self-assembled quantum dots by a magnetic-field-induced symmetry breaking, Phys. Rev. B **61**, 7273 (2000).

[38] M. Zieliński, Y. Don, and D. Gershoni, Atomistic theory of dark excitons in self-assembled quantum dots of reduced symmetry, Phys. Rev. B **91**, 085403 (2015).

[39] M. Zieliński, Dark-bright excitons mixing in alloyed InGaAs self-assembled quantum dots, Phys. Rev. B **103**, 155418 (2021).

[40] L. Besombes, Y. Léger, L. Maingault, D. Ferrand, H. Mariette, and J. Cibert, Probing the Spin State of a Single Magnetic Ion in an Individual Quantum Dot, Phys. Rev. Lett. **93**, 207403 (2004).

[41] D. E. Reiter, T. Kuhn, and V. M. Axt, All-Optical Spin Manipulation of a Single Manganese Atom in a Quantum Dot, Phys. Rev. Lett. **102**, 177403 (2009).

[42] S. Bounouar, C. de la Haye, M. Strauß, P. Schnauber, A. Thoma, M. Gschrey, J.-H. Schulze, A. Strittmatter, S. Rodt, and S. Reitzenstein, Generation of maximally entangled states and coherent control in quantum dot microlenses, Appl. Phys. Lett. **112**, 153107 (2018).

[43] M. Bayer, A. Kuther, A. Forchel, A. Gorbunov, V. B. Timofeev, F. Schäfer, J. P. Reithmaier, T. L. Reinecke, and S. N. Walck, Electron and Hole *g* Factors and Exchange Interaction from Studies of the Exciton Fine Structure in $In_{0.60}Ga_{0.40}As$ Quantum Dots, Phys. Rev. Lett. **82**, 1748 (1999).

[44] N. H. Lindner and T. Rudolph, Proposal for Pulsed On-Demand Sources of Photonic Cluster State Strings, Phys. Rev. Lett. **103**, 113602 (2009).

[45] D. E. Reiter, T. Kuhn, and V. M. Axt, Distinctive characteristics of carrier-phonon interactions in optically driven semiconductor quantum dots, Adv. Phys.: X **4**, 1655478 (2019).

[46] S. Lüker, T. Kuhn, and D. E. Reiter, Phonon impact on optical control schemes of quantum dots: Role of quantum dot geometry and symmetry, Phys. Rev. B **96**, 245306 (2017).

[47] A. Krügel, V. M. Axt, T. Kuhn, P. Machnikowski, and A. Vagov, The role of acoustic phonons for Rabi oscillations in semiconductor quantum dots, Appl. Phys. B **81**, 897 (2005).

[48] A. Vagov, M. D. Croitoru, M. Glässl, V. M. Axt, and T. Kuhn, Real-time path integrals for quantum dots: Quantum dissipative dynamics with superohmic environment coupling, Phys. Rev. B **83**, 094303 (2011).

[49] M. Glässl, A. Vagov, S. Lüker, D. E. Reiter, M. D. Croitoru, P. Machnikowski, V. M. Axt, and T. Kuhn, Long-time dynamics and stationary nonequilibrium of an optically driven strongly confined quantum dot coupled to phonons, Phys. Rev. B **84**, 195311 (2011).

[50] A. Vagov, M. D. Croitoru, V. M. Axt, P. Machnikowski, and T. Kuhn, Dynamics of quantum dots with strong electron phonon coupling: Correlation expansion vs. path integrals, Phys. Status Solidi B **248**, 839 (2011).

[51] T. Kaldewey, S. Lüker, A. V. Kuhlmann, S. R. Valentin, J.-M. Chauveau, A. Ludwig, A. D. Wieck, D. E. Reiter, T. Kuhn, and R. J. Warburton, Demonstrating the decoupling regime of the electron-phonon interaction in a quantum dot using chirped optical excitation, Phys. Rev. B **95**, 241306(R) (2017).

[52] A. Carmele and S. Reitzenstein, Non-Markovian features in semiconductor quantum optics: Quantifying the role of phonons in experiment and theory, Nanophotonics **8**, 655 (2019).

[53] P. Borri, W. Langbein, S. Schneider, U. Woggon, R. L. Sellin, D. Ouyang, and D. Bimberg, Ultralong Dephasing Time in InGaAs Quantum Dots, Phys. Rev. Lett. **87**, 157401 (2001).

[54] A. J. Ramsay, T. M. Godden, S. J. Boyle, E. M. Gauger, A. Nazir, B. W. Lovett, A. M. Fox, and M. S. Skolnick, Phonon-Induced Rabi-Frequency Renormalization of Optically Driven Single InGaAs/GaAs Quantum Dots, Phys. Rev. Lett. **105**, 177402 (2010).

[55] T. Seidelmann, F. Ungar, A. M. Barth, A. Vagov, V. M. Axt, M. Cygorek, and T. Kuhn, Phonon-Induced Enhancement of Photon Entanglement in Quantum Dot-Cavity Systems, Phys. Rev. Lett. **123**, 137401 (2019).

[56] S. Lüker, K. Gawarecki, D. E. Reiter, A. Grodecka-Grad, V. M. Axt, P. Machnikowski, and T. Kuhn, Influence of acoustic phonons on the optical control of quantum dots driven by adiabatic rapid passage, Phys. Rev. B **85**, 121302(R) (2012).

[57] P. Machnikowski and L. Jacak, Resonant nature of phonon-induced damping of Rabi oscillations in quantum dots, Phys. Rev. B **69**, 193302 (2004).

[58] T. H. Stievater, X. Li, D. G. Steel, D. Gammon, D. S. Katzer, D. Park, C. Piermarocchi, and L. J. Sham, Rabi Oscillations of Excitons in Single Quantum Dots, Phys. Rev. Lett. **87**, 133603 (2001).

[59] A. Ramsay, A review of the coherent optical control of the exciton and spin states of semiconductor quantum dots, Semicond. Sci. Technol. **25**, 103001 (2010).

[60] M. Syperek, J. Andrzejewski, W. Rudno-Rudziński, G. Sęk, J. Misiewicz, E. Pavelescu, C. Gilfert, and J. P. Reithmaier, Influence of electronic coupling on the radiative lifetime in the (In, Ga) As/GaAs quantum dot–quantum well system, Phys. Rev. B **85**, 125311 (2012).